Search for Dark Matter with top quarks at the High Luminosity-LHC

Hassan Moussawi

Deutsches Elektronen-Synchrotron, Notkestraße 85, 22607 Hamburg, Germany

E-mail: hassan.moussawi@etu.univ-lyon1.fr

September 5, 2018

Abstract

A search for weakly interacting massive dark-matter particles (WIMP DM) produced in association with top quarks is presented. Final states containing top quarks and missing transverse momentum are considered. The analysis is optimized for 3 ab^{-1} of pp collisions at a centre-of-mass energy of $\sqrt{s}$=14 TeV expected to be collected at the High-Luminosity LHC. A new set of selections optimized for the High-Luminosity LHC dataset has been proposed.

This work focuses on a sample of dileptonically decaying $t\bar{t}$ pairs. The results are interpreted in the framework of simplified models of spin-0 mediators assuming a DM candidate mass of 1 GeV and indicate that the DM signal yield, associated to a scalar DM-mediator of 100 GeV, is larger enough than the SM background yield. This result is sufficient and improve the validity of the proposal cuts.

Keywords : *WIMP, top quarks, dileptonically, pp collisions, mediator mass*

Acknowledgements

In the preamble of this report, I wish to express my sincere thanks to those who supported me during this year: Pr. Imad, Brigitte, Antonio, Nour-Mélanie, Léo, Jim, Savitri and Loïc. This work has been carried out in the ATLAS group at the Deutsches Elektronen-Synchrotron (DESY)−Hamburg, Germany.

First of all, I would like to acknowledge my supervisor Federico Meloni and the whole ATLAS group for the guidance and support during the past months. I also acknowledge Sabine Krohn and Claire David for the help with computer related issues. Special thanks go to DESY summer student organizers.

Finally, warm thanks to my parents for their unwavering support during the course of my studies. Living away from home, made me realize how much their love and support mean to me.

Contents

1 Introduction

The problem of the dark matter (DM) in the universe is, along with the explanation of "dark energy", one of the major still unsolved problems of contemporary cosmology, astrophysics and particle physics. There have been several extensive reviews over the last 15 years [1, 2, 3]. The currently most accurate, although somewhat indirect, determination of DM abundance comes from global fits of cosmological parameters to a variety of observations [4, 5], while the nature of DM remains largely unknown. Unlike normal matter, DM does not interact via the electromagnetic force. This is means it does not absorb, reflect or emit light, making it extremely hard to spot. In fact, researchers have been able to infer the existence of dark matter only from the gravitational effect it seems to have on visible matter. Dark matter seems to outweigh visible matter roughly six to one, making up about 27 % of the universe.

In order to connect observations to micro-physical models one needs a general framework within which to interpret the observations of direct detection experiments. For quite some time the prevailing method of analyzing dark matter-nucleus interactions has been to assume that dark matter is a weakly interacting massive particle (WIMP), and then to categorize the interactions as elastic and isospin conserving and either spin-independent or spin-dependent [6].

At the Large Hadron Collider (LHC), one can search for WIMP DM (χ) pair production in pp collisions. WIMP DM would not be detected and its production leads to a momentum imbalance in the detector.

Recently proposed simplified benchmark models for DM production assume the existence of a mediator particle which couples both to the Standard Model (SM) and the dark sector [7, 8, 9]. Many of these presented searches focused on the case of a fermionic DM produced through the exchange of a spin-0 mediator, which can be either a colour-neutral scalar or pseudoscalar particle (denoted by ϕ or a, respectively). The couplings of the mediator to the SM fermions are severely restricted by precision flavour measurements. In fact, according to the Minimal Flavour Violation [10], the interaction between any new neutral spin-0 state and SM matter is proportional to the fermion masses via Yukawa-type couplings[1].

This report focuses on DM produced in association with heavy flavour top quarks:

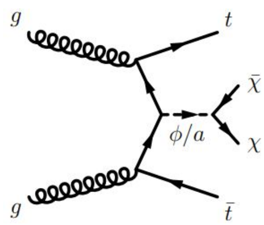

Figure 1: Feynman diagram at the lowest order for spin-0 mediator: colour-neutral spin-0 mediator associated production with top quarks $t\bar{t} + \phi/a$.

[1]The couplings to W and Z bosons are set to zero in these simplified models. In addition, the coupling of the mediator to the dark sector are not taken to be proportional to the mass of the DM candidates.

For signatures, final states where both W bosons decay into leptons are considered in this analysis. Representative Feynman diagram for the production of this model is shown in Figure 1: the model has four parameters: the mass of the mediator m_ϕ or m_a, the DM mass m_χ, the DM-mediator couplings g_χ, and the flavour-universal SM-mediator coupling g_q. The mediator can decay into SM particles or into DM particles. This study is sensitive to decays of the mediator into a pair of DM particles.

2 Definition of the MET and M_{T2} variables

The two important variables used in the analysis are discussed here.

2.1 Missing transverse momentum MET

All the detectors at the LHC have been designed to cover as much solid angle as practically possible with calorimetry. The primary motivation of this is to provide as complete of a picture as possible of the event, including the presence of one or more energetic neutrinos or other weakly-interacting stable particles though apparent missing energy. The unknown longitudinal momentum of the interacting partons makes it impossible to exploit energy conservation along the beam direction. However, the transverse energy balance can be measured with an accuracy good enough to help establish a physics signature involving one or more non-interacting particles.

The MET can referred to the energy that is not detected in a particle detector, but is expected due to the laws of conservation of energy and conservation of momentum. It's used to infer the presence of non-detectable particles that do not interact via the electromagnetic or strong interactions and thus are not detectable in LHC experiments. These particles are most notably neutrinos or DM particles. MET can be defined as:

$$\vec{E}_{\mathrm{T}}^{miss} = -\Big(\sum_i \vec{p}_{\mathrm{T}}(i)\Big), \tag{1}$$

Where $\vec{p}_{\mathrm{T}}(i)$ is the transverse momentum of each visible particle.

2.2 M_{T2} variable

The kinematic mass variable M_{T2} is introduced to measure the mass of pair-produced particles in situations where both particles decay to a final state containing an undetected DM particle χ of mass m_χ. For each decay chain, the visible system is defined by the transverse momentum $\vec{p}_{\mathrm{T}}^{vis(i)}$, transverse energy $E_{\mathrm{T}}^{vis(i)}$, and mass $m^{vis(i)}$ $(i = 1, 2)$ obtained by summing the four-momenta of all detected particles in the decay chain. The two visible systems are accompanied by the two undetected particles with unknown transverse momentum $\vec{p}_{\mathrm{T}}^{\chi(i)}$. In analogy with the transverse mass used for the W-boson mass determination [11], two transverse masses are defined for the two pair-produced particles:

$$(M_{\mathrm{T}}^{(i)})^2 = (m^{vis(i)})^2 + m_\chi^2 + 2\Big(E_{\mathrm{T}}^{vis(i)} E_{\mathrm{T}}^{\chi(i)} - \vec{p}_{\mathrm{T}}^{\chi(i)} \cdot \vec{p}_{\mathrm{T}}^{vis(i)}\Big) \tag{2}$$

If the correct values of m_χ, $\vec{p}_{\mathrm{T}}^{\chi(i)}$, $m^{vis(i)}$ and $\vec{p}_{\mathrm{T}}^{vis(i)}$ are chosen, the transverse masses $M_{\mathrm{T}}^{(i)}$ do not exceed the mass of the parent particles. However, the momentum $\vec{p}_{\mathrm{T}}^{\chi(i)}$ of the unseen particles are not experimentally accessible individually. Only their sum, the missing transverse momentum $\vec{p}_{\mathrm{T}}^{miss}$, is known. A generalization of the transverse mass, the M_{T2} variable, is then defined as:

$$M_{\mathrm{T2}}(m_\chi) = \min_{\vec{p}_{\mathrm{T}}^{\chi(1)}+\vec{p}_{\mathrm{T}}^{\chi(2)}=\vec{p}_{\mathrm{T}}^{miss}} \left[\max\left(M_{\mathrm{T}}^{(1)} + M_{\mathrm{T}}^{(2)}\right) \right], \tag{3}$$

Where the DM mass m_χ is a free parameter fixed at 1 GeV in the case of the analysis. The minimization is performed over trial momentum of the undetected particles fulfilling the $\vec{p}_{\mathrm{T}}^{miss}$ constraint.

3 Analysis strategy

In this section a summary of the pre-selection cuts applied to the analyzed DM sample is presented, together with the considered optimisation strategy.

3.1 Significance

The concept of the statistical significance Z_n is formally introduced as the probability of the background fluctuating to or above the sum of the expected number of signal events and background events $N_s + N_b$ averaged over uncertainty $\pm\delta_b N_b$ around N_b:

$$Z_n(N_s, N_b, \delta_b) = \sqrt{2}\,\mathrm{erf}^{-1}(1 - 2p), \tag{4}$$

and

$$p = \int_0^\infty db\; g(b; N_b, \delta_b N_b) \sum_{i=N_s+N_b}^{\infty} P(i; b), \tag{5}$$

Where δ_b is the fractional uncertainty on N_b, g and P are the probability density functions (PDFs) of the Gaussian and Poisson distributions, respectively.

Equation 4 above transforms p to the equivalent number of σ ($n\sigma$) of the Gaussian distribution. Note that, Z_n can be also written as a smooth function of N_s and N_b. The significance was estimated using the `BinomialExpZ` in `RooStats` with a relative background uncertainty of 20 %.

3.2 Event selection

The event selection is designed using simulated samples of background and signal processes. SRt3, defined in [12] has been optimized to detector dark-matter production via spin-0 mediator in association with a $t\bar{t}$ pair. This selection has been used as starting point to define a new set of cuts optimized for the High-Luminosity LHC dataset.

3.2.1 Signatures with top quarks

To discriminate between the DM signal and the SM background, the following requirements are implemented. Table 1 below summarizes the SRt3 selection criteria.

Observable	Requirement
Trigger	2ℓ
N_j	≥ 1
N_b^{M}	≥ 1
N_ℓ^{M}	2 OS
$p_{\mathrm{T}}(bj_1)$ [GeV]	> 30
$p_{\mathrm{T}}(j_1, j_2)$ [GeV]	> 30
$p_{\mathrm{T}}(\ell_1, \ell_2)$ [GeV]	$> 25, 20$
$m_{\ell\ell}$ [GeV]	> 20
$\lvert m_{\ell\ell}^{\mathrm{SF}} - m_Z\rvert$ [GeV]	> 20
$\Delta\phi_{boost}$ [rad]	< 0.8
$m_{b2\ell}^{min}$ [GeV]	< 170
ξ^+ [GeV]	> 170
$m_{\mathrm{T2}}^{\ell\ell}$ [GeV]	> 100

Table 1: Summary of the final kinematic selections for the signal region SRt3.

The events are required to have exactly two opposite-sign leptons, either same- or different-flavour, with an invariant mass, $m_{\ell\ell}$, being larger than 20 GeV. In addition, for same-flavour lepton pairs, events with $m_{\ell\ell}$ within 20 GeV of the Z-boson mass are vetoed. Furthermore, the requirement on the two-lepton triggers and the leading and sub-leading lepton transverse momentum in the event to be at least 25 and 20 GeV, respectively, ensures that the plateau of efficiency of the triggers is reached. The reducible backgrounds (dileptonic $t\bar{t}$ decays, Z + jets and dibosons) are rejected using the lepton-based "stransverse mass", $m_{\mathrm{T2}}^{\ell\ell}$, which is a kinematic variable with an endpoint at the W-boson mass for events containing two W bosons decaying into leptons. However, a linear combination with the E_{T}^{miss} is also used in this selection, in order to maximize the discrimination power:

$$\xi^+ = m_{\mathrm{T2}}^{\ell\ell} + 0.2E_{\mathrm{T}}^{miss} \tag{6}$$

Some additional pre-selections on the azimuthal angular distance between $\vec{p}_{\mathrm{T}}^{\mathrm{miss}}$ and the vector sum of $\vec{p}_{\mathrm{T}}^{\mathrm{miss}}$ and the transverse momentum of the leptons, $\Delta\phi_{boost}$ and the $m_{b2\ell}^{min}$ are applied. These variables help to reject residual contamination from reducible backgrounds.

Figure 2 below shows the distributions of the most interesting variables with the significance panel (Z_n) after applying the pre-selection cuts discussed among. For each distribution, the background expectation (filled coloured histograms) from different processes and a benchmark DM signal (red line) with a scalar mediator of 100 GeV are presented. The MET and M_{T2} distributions show that the SM events have high values of MET or M_{T2} (up to 800 GeV for the MET and 340 GeV for the M_{T2}). $t\bar{t}+V$ events, and in particular $t\bar{t}+Z$ events where the Z boson decays into neutrinos, represent the irreducible background for this targeting SRt3 DM production. The next-most important background is from $t\bar{t}$ events where the W-bosons decay dileptonically into a lepton and neutrino. Furthermore, the background from $Z(\nu\bar{\nu})$ + jets and other SM processes is small.

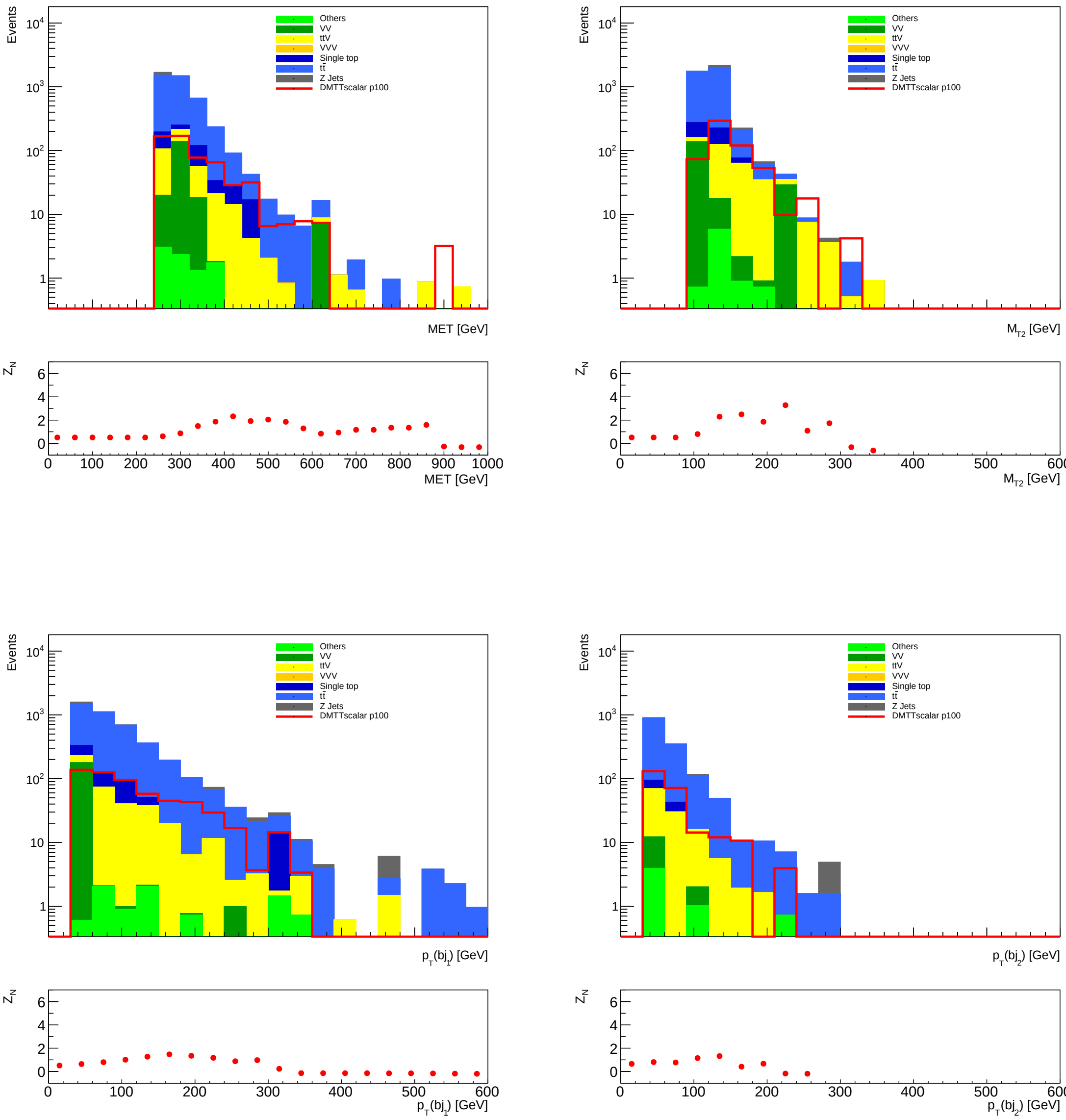

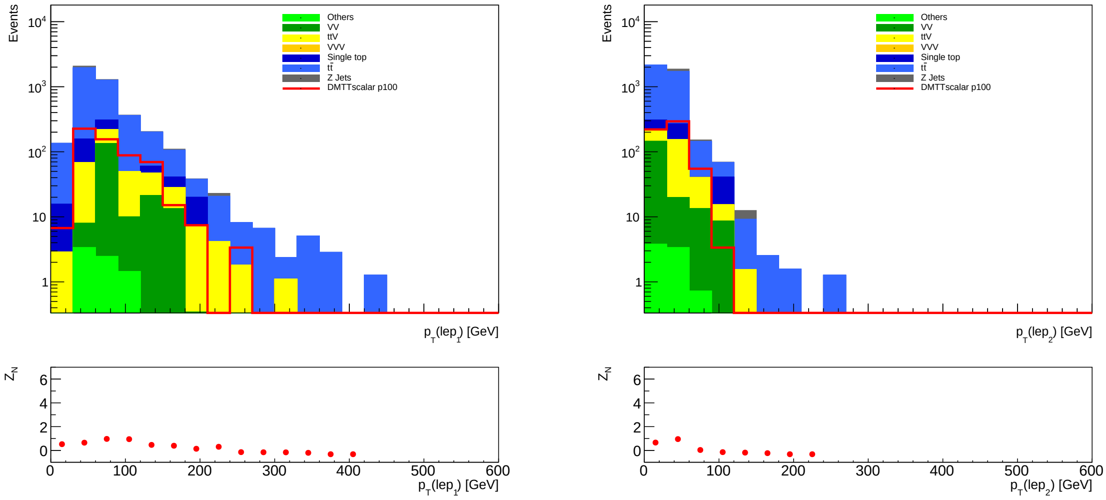

Figure 2: Comparison of the data after the pre-selection cuts of some kinematic distributions in the SRt3. The bottom panel shows the significance Z_n. The last bins include overflows, where applicable. The top left panel shows the MET distribution. The MET requirement is relaxed to 240 GeV. The other panels show the $\mathrm{M_{T2}}$ distribution (top right), the $p_{\mathrm{T}}(bj_1)$ distribution (middle left), the $p_{\mathrm{T}}(bj_2)$ distribution (middle right), the $p_{\mathrm{T}}(\ell_1)$ distribution and the $p_{\mathrm{T}}(\ell_2)$ distribution in the same SR.

4 Optimization strategy

The significance Z_n as defined in 3.1 is usefully needed for the optimization of the final selection cuts. For this purpose, several steps are combined. These steps are based on the expected counts of the background and DM signal, given by integrating Z_n to the left or the right of a cut on the bin edge depending on the considered variable.

4.1 Choice of the final cuts

To assure the quality of the final cuts, the (N - 1) plots technique is used. As a first step, a set of selections has been decided by taking the maximal value of the significance for each discriminating variable. The results of this first step are summarized in Table 2. Then, every kinematic discriminant is studied after applying all the selections, but for the one on the variable itself. The choice for the final selection cut is possibly adjusted according to the new maximum significance. The results of this second step are summarized in Table 3.

The total background and DM signal of these observables have been integrated to the right, it assures a high values of significance compared to the others options. Figure 3 below shows the (N - 1) plots. At this stage, the new maximal values of the Z_n plots are taken to make up the new selection cuts.

Observable	Requirement
M_{T2} [GeV]	≥ 150
$p_{\mathrm{T}}(bj_1)$ [GeV]	≥ 105
$p_{\mathrm{T}}(bj_2)$ [GeV]	≥ 75

Table 2: Summary of the kinematic cuts on the maximal values of the significance in the signal region SRt3.

Observable	Requirement
M_{T2} [GeV]	≥ 170
$p_{\mathrm{T}}(bj_1)$ [GeV]	≥ 137
$p_{\mathrm{T}}(bj_2)$ [GeV]	≥ 47

Table 3: Summary of the final kinematic cuts in the signal region SRt3.

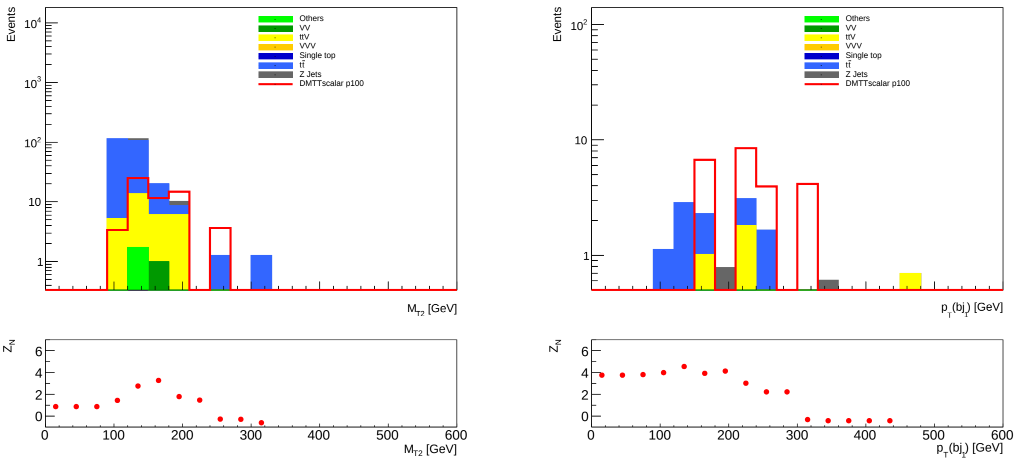

The (N - 1) plots show that all the distributions are dominated by the DM signal, $t\bar{t}$ SM events and $t\bar{t} + Z$ SM events.

Figure 4 shows the distribution of the various variables after applying the final cuts. The plots, compared to the situation before the optimization is done, show more DM signal events. The total SM background events are also reduced. Events from $t\bar{t} + Z$ and $t\bar{t}$ are the most important. Z + jets events have a small contribution. The MET distribution shows that the SM processes with two leptons from Z bosons tend to have large values of MET (540 GeV) and $\mathrm{M_{T2}}$ (320 GeV). Furthermore, the events number for the p_{T} distributions of leptons and b-jets is higher than those for the MET and $\mathrm{M_{T2}}$ distribution. Nevertheless, the significance panel shows large values of Z_n.

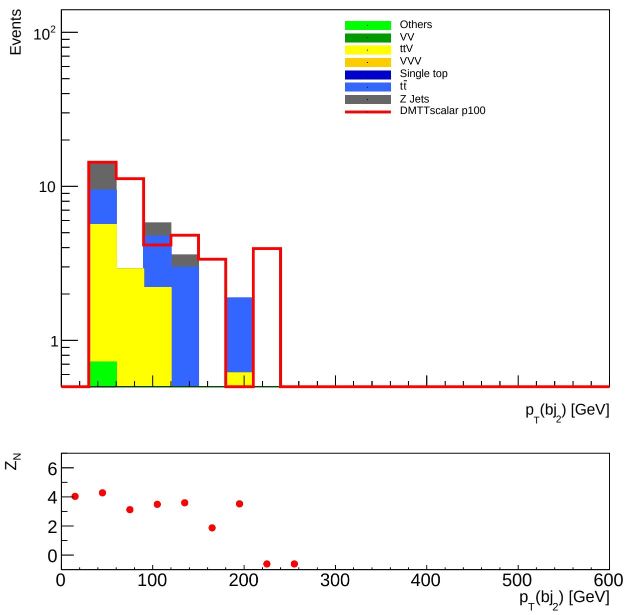

Figure 3: (N - 1) plots in the SRt3. The bottom panel shows a maximal value of significance Z_n. The top left panel show the $\mathrm{M_{T2}}$ distribution. The other panels show the $p_{\mathrm{T}}(bj_1)$ distribution (top right), the $p_{\mathrm{T}}(bj_2)$ distribution (middle) in the same SR.

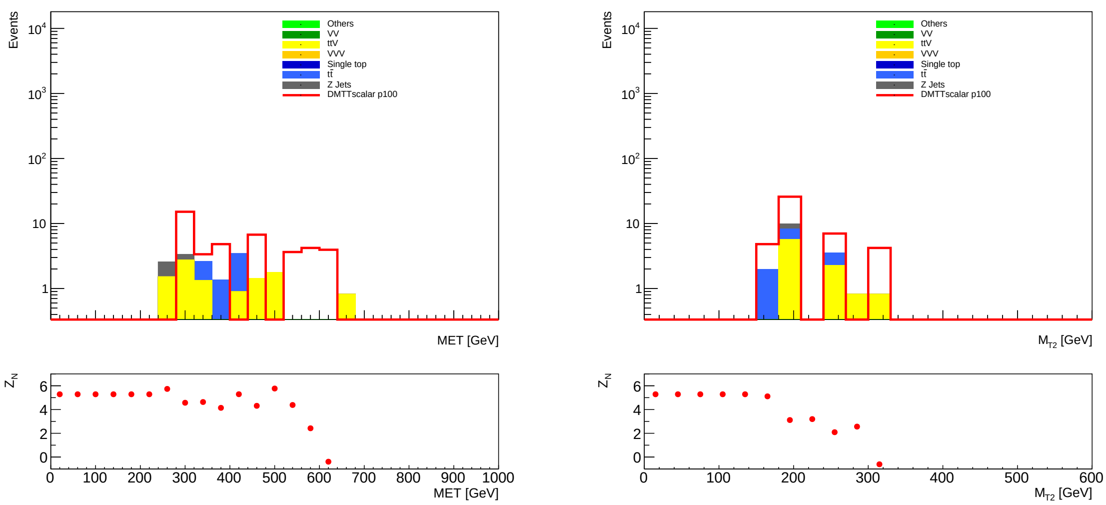

5 Results

The expected yields in the signal region of this analysis are reported in Table 4. The expected signal yields for the selected benchmark model for scalar mediator are

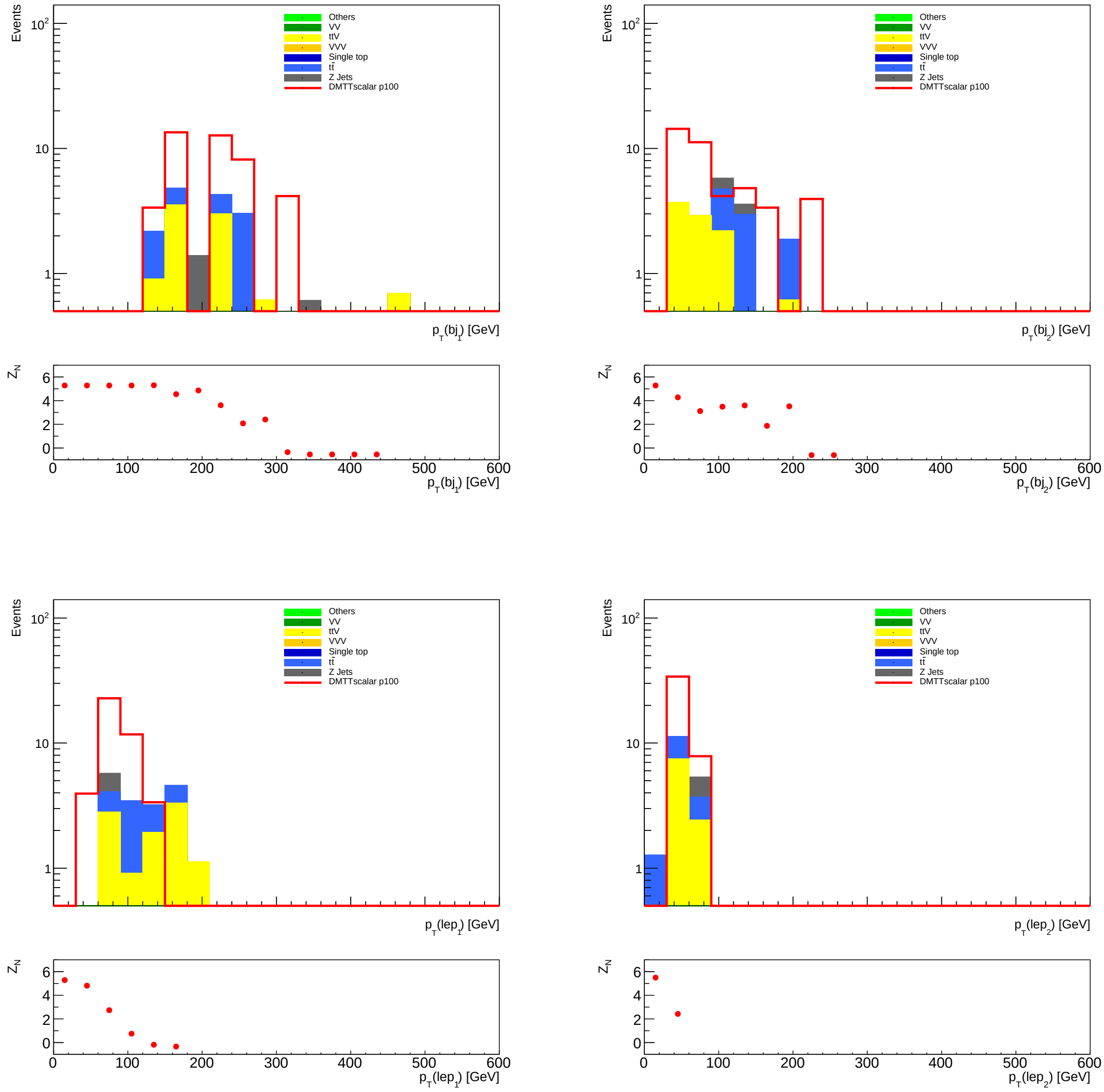

Figure 4: Comparison of the data after the final selection cuts of some kinematic distributions in the SRt3. The bottom panel shows the significance Z_n. The top left panel shows the MET distribution. The other panels show the M_{T2} distribution (top right), the $p_T(bj_1)$ distribution (middle left), the $p_T(bj_2)$ distribution (middle right), the $p_T(\ell_1)$ distribution and the $p_T(\ell_2)$ distribution in the same SR.

also shown. The uncertainties in the yields include the statistical uncertainty in the theoretical modeling of the SM background processes. The DM signal with a mediator mass of 100 GeV shows an expected yield up to 45 events. Compared to the total SM background yield, this value is sufficient and can improve the validity of the proposal optimization cuts.

Total background	33.05 ± 6.9
$t\bar{t}$ and Wt	11.44 ± 3.81
$t\bar{t} + Z$	14.41 ± 4.46
Z + jets	6.38 ± 3.55
VV	0.05 ± 0.05
VVV	0.04 ± 0.04
Others	0.72 ± 0.72
Signal benchmark	
$m(\phi, \chi) = (100, 1)$ GeV	45.79 ± 13.31

Table 4: Expected yields in the re-optimised SR for 3 ab^{-1} of pp collisions. SM processes with negligible contributions are indicated as Others. Benchmark signal models yields are also given for this SR. The uncertainties in the yields include statistical uncertainties from MC generation.

6 Conclusions and outlook

This work reports a prospect for a search for dark-matter pair production in association with top quarks. The analysis is optimized for 3 ab^{-1} of pp collisions at a centre-of-mass energy of $\sqrt{s} = 14$ TeV expected to be collected at the High-Luminosity LHC. A new set of selections optimized for the High-Luminosity LHC dataset has been defined. Preliminary results indicate that the DM signal yield is larger enough than the SM background yield.

This work motivates a future study of the exclusion limits for colour-neutral $t\bar{t} + \phi$ scalar model as a function of the mediator mass for a DM mass of 1 GeV. The limits should be calculated at 95 % CL and be expressed in terms of the ratio of the excluded cross-section to the nominal one for a coupling assumption of $g = g_q = g_\chi = 1$.

References

[1] G. Jungman, M. Kamionkowski and K. Griest, Phys. Rept. 267 (1996) 195 [hep-ph/9506380].

[2] L. Bergstrom, Rept. Prog. Phys. 63 (2000) 793 [hep-ph/0002126].

[3] G. Bertone, D. Hooper and J. Silk, Phys. Rept. 405 (2005) 279 [hep-ph/0404175].

[4] E. Komatsu et al., Seven-Year Wilkinson Microwave Anisotropy Probe (WMAP) Observations: Cosmological Interpretation, Astrophys. J. Suppl. 192 (2011) 18, arXiv: 1001.4538 [astro-ph.CO].

[5] P. A. R. Ade et al., Planck 2015 results. XIII. Cosmological parameters, Astron. Astrophys. A 594 (2016) 13, arXiv: 1502.01589 [astro-ph.CO].

[6] G. Steigman and M. S. Turner, Cosmological constraints on the properties of Weakly Interacting Massive Particles, Nucl. Phys. B 253 (1985) 375.

[7] D. Abercrombie et al., Dark matter benchmark models for early LHC run-2 Searches: Report of the ATLAS/CMS Dark Matter Forum, 2015, arXiv: 1507.00966 [hep-ex].

[8] M. R. Buckley, D. Feld, and D. Goncalves, Scalar simplified models for dark matter, Phys. Rev. D 91 (2015) 015017, arXiv: 1410.6497 [hep-ph].

[9] U. Haisch and E. Re, Simplified dark matter top-quark interactions at the LHC, JHEP 06 (2015) 078, arXiv: 1503.00691 [hep-ph].

[10] G. DAmbrosio, G. F. Giudice, G. Isidori, and A. Strumia, Minimal flavor violation: An Effective field theory approach, Nucl. Phys. B 645 (2002) 155, arXiv: hep-ph/0207036.

[11] UA1 Collaboration, Experimental observation of isolated large transverse energy electrons with associated missing energy at $\sqrt{s} = 540$ GeV, Phys. Lett. B 122 (1983) 103, doi:10.1016/0370-2693(83)91177-2.

[12] Aaboud, M., Aad, G., Abbott, B. et al. Eur. Phys. J. C (2018) 78. https://doi.org/10.1140/epjc/s10052-017-5486-1.